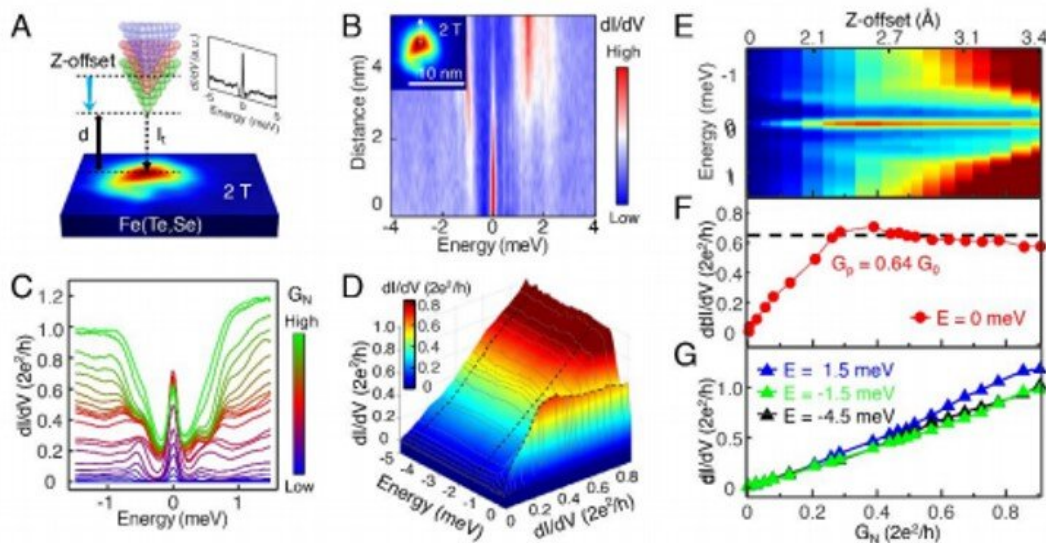


Nearly quantized conductance plateau of vortex mode in an iron-based superconductor

December 31 2019, by Thamarasee Jeewandara



Zero-bias conductance plateau observed on FeTe_{0.55}Se_{0.45}. (A) A schematic of variable tunnel coupling STM/S method. A zero-bias conductance map under 2.0 T is shown on a sample surface. A dI/dV spectrum measured at the center of the vortex core ($V_s = -5$ mV, $I_t = 500$ pA, $V_{mod} = 0.02$ mV) is shown in the right-top inset, a sharp zero-bias conductance peak (ZBCP) is observed. When the tunneling current (I_t) is adjusted by the STM regulation loop, the tunnel coupling between the STM tip and the MZM can be tuned continuously by the tip-sample distance (d). Larger tunnel coupling corresponds to smaller d and larger tunneling-barrier conductance ($G_N = I_t/V_s$, V_s is the setpoint voltage). Z-offset can be read out simultaneously, which indicates the absolute z-direction motion of the STM tip. (B) A line-cut intensity plot along the dashed white arrow in the inset, measured from the same vortex shown in (A), showing a stable MZM

across the vortex core. (C) An overlapping plot of dI/dV spectra under different tunnel coupling values parameterized in GN. The blue curve is measured under the smallest GN while the green curve with the largest GN. (D) A three-dimensional plot of tunnel coupling dependent measurement, $dI/dV(E, GN)$. For clarity, only the data points in the energy range of $[-5.0, 0.2]$ meV are shown. (E) A color-scale plot of (C) within the energy range of $[-1.5, 1.5]$ meV that expands the spectra as a function of GN. The z-offset information, which was taken simultaneously by STM, is also labeled at the upper axis. The maximum distance the tip approached is 3.4 \AA . (F) A horizontal line-cut at the zero-bias from (E). The conductance curve shows a plateau behavior with its plateau conductance (GP) equal to $(0.64 \pm 0.04) G_0$. (G) Horizontal line-cuts at high-bias values from (E). The absence of a conductance plateau on these curves indicates the conventional tunneling behavior at the energy of continuous states. All data are measured at $T_{\text{eff}} = 377 \text{ mK}$. Credit: *Science*, doi: 10.1126/science.aax0274

When a semiconducting nanowire is coupled to a [superconductor](#), it can be tuned to topological quantum states thought to host [localized quasiparticles](#) known as Majorana Zero Modes (MZM). MZMs are their own [antiparticles](#), with promising applications in [topological quantum computing](#). Due to particle-antiparticle equivalence, MZMs exhibit [quantized conductance](#) at low temperatures. While many theoretical proposals exist to realize MZMs in solid state systems, their experimental realization is confronted by non-idealities.

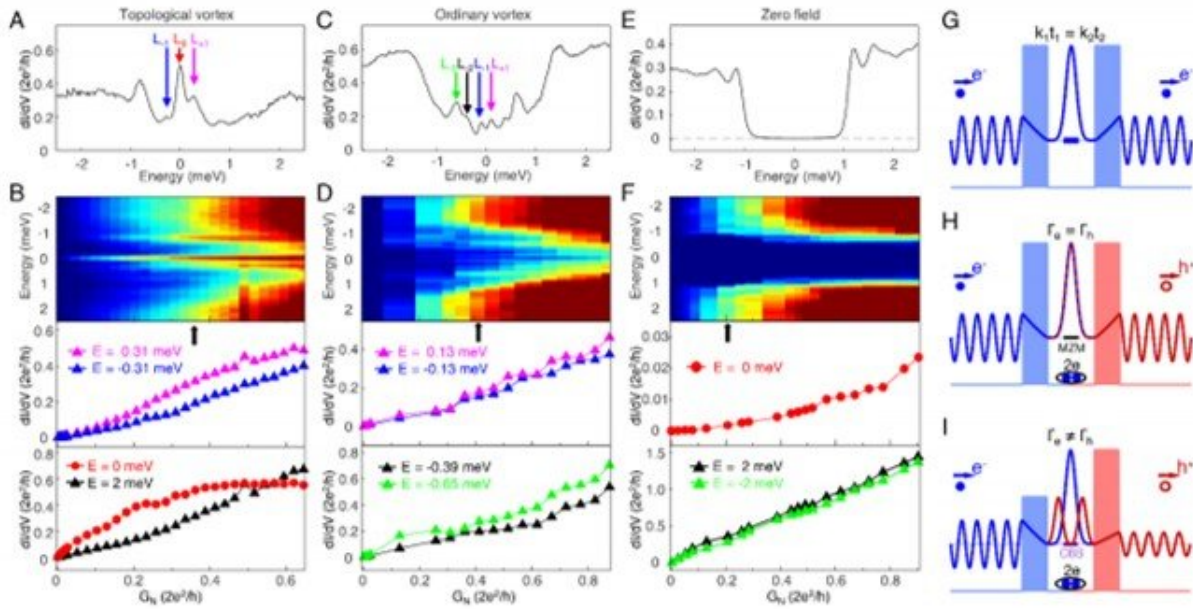
In a new report in *Science*, Shiyu Zhu and a team of interdisciplinary researchers in China and the U.S. used variable-tunnel-coupled [scanning tunneling spectroscopy](#) to study tunneling conductance of [vortex bound states](#) of superconductors. For instance, superconductors have a "gap" in energy in the absence of electron states—so electrons cannot tunnel in, whereas at a [vortex line](#) the [magnetic field](#) will close the gap to form electron states. The researchers reported observations with $\text{FeTe}_{0.55}\text{Se}_{0.45}$ superconductors, where they recorded conductance plateaus as a

function of tunneling coupling for zero-energy vortex bound states, with values close to, and even reaching, the universal [quantum conductance](#) value $2e^2/h$; where e , is the electron charge and h is [Planck's constant](#). In contrast, they did not observe plateaus on either finite energy vortex bound states or within the continuum of electronic states outside the superconducting gap. This behavior of zero-mode conductance supported the existence of MZMs in $\text{FeTe}_{0.55}\text{Se}_{0.45}$ crystals.

Majorana Zero Modes (MZMs) obey [non-Abelian statistics](#) i.e. excitations beyond the usual fermionic or bosonic modes of excitation, to play an extremely [important role in quantum computation](#). In the past two decades, physicists predicted MZMs within [p-wave superconductors](#) and spin-orbit-coupled [materials proximitized](#) (to realize properties of a material absent from any constituent region of the heterostructure), by [s-wave superconductors](#). Researchers had observed experimental evidence for MZMs in various systems including [semiconductor-superconductor nanowires](#), topological insulator-[superconductor heterostructures](#) and atomic chains on [superconducting substrates](#). Physicists and materials scientists have also recently developed fully gapped bulk iron-based superconductors as a [single-material platform](#) to realize MZMs. Subsequently, they found [evidence for MZMs](#) in topological vortices on the surface of $\text{FeTe}_{0.55}\text{Se}_{0.45}$ crystals using scanning tunneling microscopy/spectroscopy (STM/S).

The conductance of an MZM can exhibit a quantized plateau at sufficiently low temperatures at the value of $2e^2/h$; where e is the electron charge and h the Planck's constant. This quantized Majorana conductance results from perfect resonant [Andreev reflection](#)—a type of particle scattering that occurs at interfaces between a superconductor and normal state material, guaranteed by the inherent [particle-hole symmetry of MZM](#). Scientists had observed a quantized conductance plateau in an [InSb-Al nanowire system](#), consistent with [the existence of MZMs](#). Similarly, iron-based superconductors with [zero-bias](#)

[conductance peaks](#) (ZBCPs) obtained using STM/S experiments have large topological gaps and offer the possibility of observing Majorana quantized conductance, without contamination from low-lying [Caroli-de Gennes-Matricon bound states](#) (CBSs). As a result of [preceding experimental prospects](#), Zhu et al. presently employed a variable tunnel coupling STM/S method to study Majorana conductance across a large range of tip-sample distance in vortex cores of FeTe_{0.55}Se_{0.45} crystal samples.



Majorana induced resonance Andreev reflection. (A) A dI/dV spectrum measured at the center of a topological vortex ($V_s = -5$ mV, $I_t = 140$ nA, $V_{mod} = 0.02$ mV), which shows an MZM (red arrow) coexisting with a high-level CBS located at ± 0.31 meV. (B) A tunnel coupling dependent measurement on the vortex shown on (A) at 2 T. Top panel: a color-scale plot, dI/dV. The GN position of (A) is marked by a black arrow. Middle panel: tunnel coupling evolution of CBS conductance, which shows no plateau behavior. Bottom panel: tunnel coupling evolution of conductance at the energies of 0 meV (red circles, exhibiting a plateau) and 2 meV (black triangles monotonically increasing). (C)

A dI/dV spectrum measured at the center of an ordinary vortex ($V_s = -5\text{ mV}$, $I_t = 140\text{ nA}$, $V_{\text{mod}} = 0.02\text{ mV}$), which clearly shows three levels of CBS at $\pm 0.13\text{ meV}$ (magenta and blue arrows), $\pm 0.39\text{ meV}$ (black arrows) and $\pm 0.65\text{ meV}$ (green arrow). (D) Similar to (B) but measured on the vortex shown in (C). Middle and bottom panels: tunnel coupling evolution of CBS conductance, showing no plateau feature. (E) A dI/dV spectrum measured at 0 T ($V_s = -5\text{ mV}$, $I_t = 80\text{ nA}$, $V_{\text{mod}} = 0.02\text{ mV}$). A hard superconducting gap can be seen. (F) Similar to (B) and (D), but measured under 0 T. Middle panel: tunnel coupling evolution of zero-bias conductance (normal metal-superconductor junction case). Bottom panel: tunnel coupling evolution at the above gap energy (normal metal-normal metal junction case). There is no plateau behavior at 0 T. (G) A schematic of resonant tunneling through a symmetric barrier system. The wavefunction evolution of a tunnelled electron is shown. kt is penetration constant. (H) The double barrier view of the MZM-induced resonant Andreev reflection. The blue and red colors indicate the electron and hole process, respectively. The equivalence of particle and hole components in MZM ensures the same tunnel coupling on electron and hole barrier. (I) The double-barrier view of Andreev reflection mediated by a CBS. The arbitrary mixing of particle-hole components in CBS breaks the resonance condition. All data are measured at 377 mK. Credit: *Science*, doi: 10.1126/science.aax0274

The effective electron temperature of the scanning tunneling microscope (STM) was 377 mK and the researchers continuously tuned the tunnel coupling by changing the tip-sample distance, which correlated with the tunnel-barrier conductance. By applying a 2 T (Tesla) magnetic field perpendicular to the sample surface, Zhu et al. observed a sharp ZBCP (zero-bias conductance peak) at a vortex core. As expected for [an isolated MZM in a quantum-limited vortex](#), the ZBCP did not disperse or split across the vortex core. They performed tunnel-coupling dependent measurements on the observed ZBCP, by adding the STM tip at the center of a [topological vortex](#), to record a set of dI/dV spectra corresponding to the electron density of states at the position of the tip, for different tip-sample distances. They observed the ZBCP to remain as

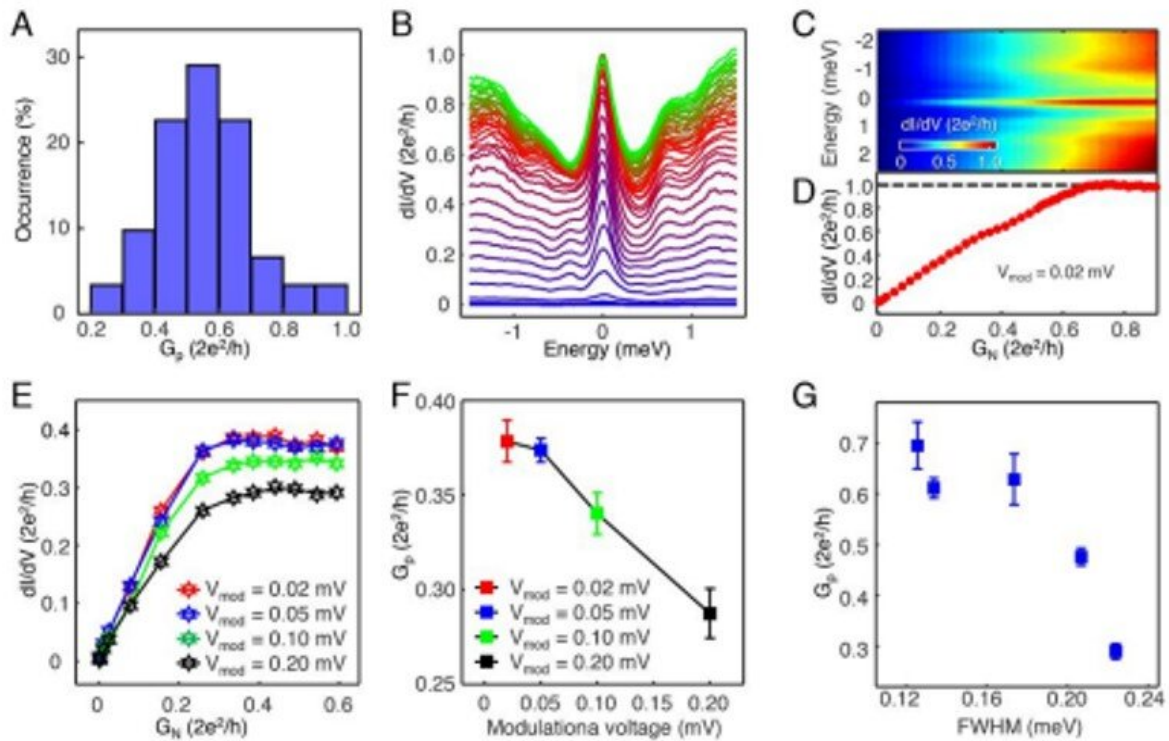
a well-defined peak located at zero energy.

To examine the particle-hole symmetry of the MZMs, they compared and contrasted the conductance behavior of zero-energy MZMs and finite-energy CBSs (Caroli-de Gennes-Matricon bound states). Zhu et al. observed two distinct types of topological and ordinary vortices with, or without MZM, which differed by a [half-integer level shift](#) of vortex bound states. They performed tunnel coupling dependent measurements on a topological vortex to show an MZM and first CBS level, at 0 meV and ± 0.3 meV, they also conducted measurements on an ordinary vortex.

When the research team repeated the experiments in zero magnetic field at the same location, they observed a hard, superconducting gap. The scientists only observed the conductance plateau feature in ZBCP, which indicated behavior unique to Majorana modes. The plateau behavior observed in the work also provided evidence for the Majorana-induced resonant Andreev reflection. Thereafter, during electron tunneling from a normal electrode through a barrier into a superconductor, the team observed the [Andreev reflection process](#) convert the incident electron into an outgoing hole within the same electrode. This resulted in a double-barrier system in the particle-hole [Hilbert space](#) (an abstract vector space in quantum mechanics).

In the case of Andreev reflection through a single MZM, equal amplitudes of particle/hole components due to particle-antiparticle equivalence of MZMs ensured identical tunnel coupling, with the electron and hole in the same electrode ($\Gamma_e = \Gamma_h$). As a result, the resonant Andreev reflection mediated through a single MZM led to a $2e^2/h$ -quantized [zero-bias conductance plateau](#). In contrast, [low-energy CBS](#) and other [trivial sub-gap states](#) do not contain Majorana symmetry and the relationship between the electron and hole is broken in a CBS-mediated Andreev reflection, causing an absence of a conductance plateau. Furthermore, when Zhu et al. removed the magnetic field in the

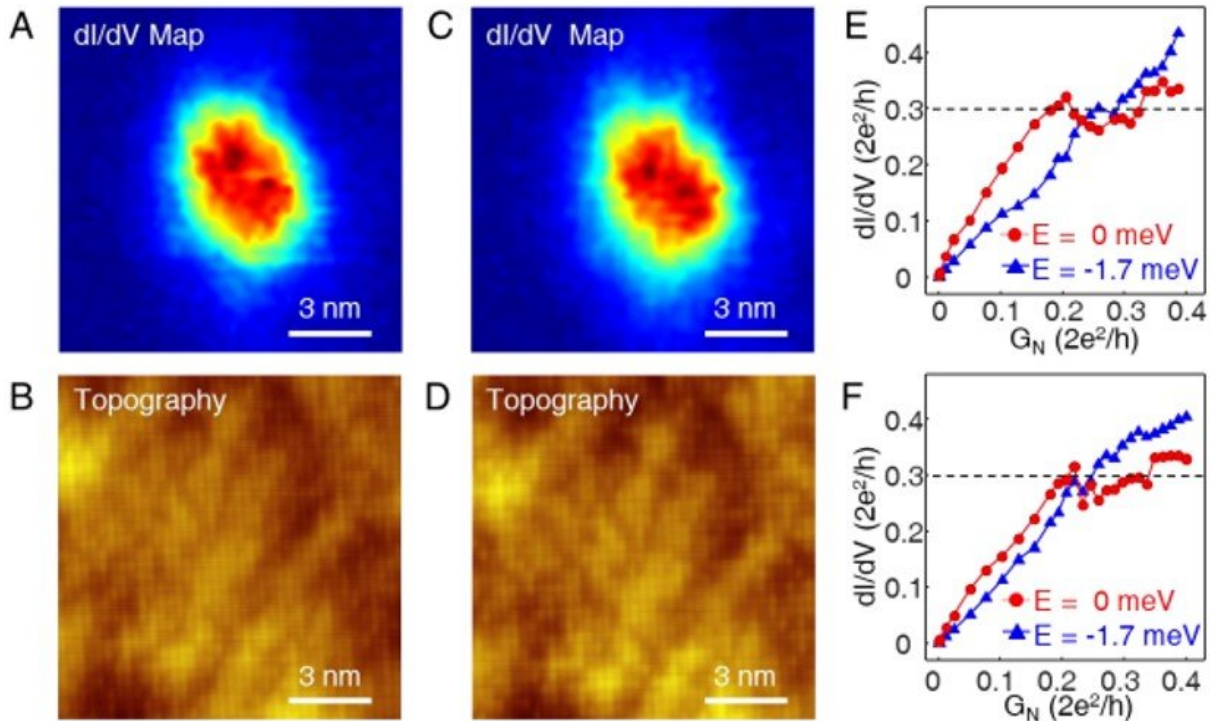
experimental system, the observed zero-bias conductance plateau in the vortex core disappeared, therefore the observations could not be credited to [quantum ballistic transport](#).



The conductance variation of Majorana plateau. (A) A histogram of the G_p from 31 sets of data which are measured with the same instrument. Sorting of the plateau conductance (G_p) in the order of increasing magnification can be found ($V_s = -5\text{ mV}$, $V_{\text{mod}} = 0.02\text{ mV}$). (B) The overlapping plot of 38 dI/dV spectra selected from a topological vortex that reached a quantized conductance plateau ($V_s = -5\text{ mV}$, $V_{\text{mod}} = 0.02\text{ mV}$). (C) A color-scale plot of (B) with the energy range of $[-2.5, 2.5]$ meV that shows the spectra as a function of G_N . (D) A horizontal line-cut at the zero-bias from (C). The conductance curve shows the conductance plateau reach G_0 . (E) A series of tunnel coupling dependent measurements on the same MZM, with four modulation voltages of 0.02 mV, 0.05 mV, 0.10 mV and 0.20 mV. (F) The plot of G_p as a function of modulation

voltage of the data shown in (E). (G) Relationship between full-wave half maximum of ZBCP and G_p , obtained from five different MZMs measured at the same experimental conditions, suggesting that the quasiparticle poisoning effect affects the plateau value. The FWHM were extracted from the spectrum measured at a large tip-sample distance with the same experimental parameters ($V_s = -5$ mV, $I_t = 500$ pA, $V_{mod} = 0.02$ mV). Credit: *Science*, doi: 10.1126/science.aax0274

The scientists observed the plateau behavior of ZBCPs repeatedly in many topological vortices across 60 measurements. To understand the effects of instrumental broadening on Majorana conductance plateaus, the scientists varied the modulation voltage (V_{mod}). This allowed them to study the V_{mod} -evolution of Majorana conductance plateaus on a given topological vortex. Zhu et al. then tested the reversibility of the process by varying tunneling coupling in STM. They found that both topography and the conductance plateau could be reproduced after two repeated sequences to indicate the absence of irreversible damage of the tip and sample during measurements. The research team require further theoretical efforts to gather complete understanding of the experiments, as they did not exclude other mechanisms related to zero-bias conductance plateaus.



Reversibility of tunnel coupling dependent measurements. (A)-(B) A zero-bias dI/dV map and corresponding STM topography measured before tunnel coupling dependent measurements. The map and the topography are measured at the same area. The magnetic field is 2.0 T. (C)-(D) A zero-bias dI/dV map and corresponding STM topography measured after tunnel coupling dependent measurements. The magnetic field is 2.0 T. The measuring parameters are the same with the ones in (A-B): sample bias, $V_s = -5$ mV; tunneling current, $I_t = 500$ pA. (E)-(F) Two repeated sequences of tunnel coupling dependent measurements at the same spatial position, showing an average plateau conductance of $0.30 G_0$, respectively. The data shown in (F) are recorded during a second tip-approaching process after finishing the first one. Credit: *Science*, doi: 10.1126/science.aax0274

In this way, the observation of a zero-bias conductance plateau in an experimental two-dimensional vortex approached the quantized conductance value of $2e^2/h$. In this work, Shiyu Zhu and colleagues

provided spatially-resolved spectroscopic evidence for Majorana-induced resonant electron transmission into a bulk superconductor. The results move a step further toward applications of [braiding operators](#) to describe topological entanglements [or universal quantum gates](#) for topological quantum computation.

More information: 1. Nearly quantized conductance plateau of vortex zero mode in an iron-based superconductor [science.sciencemag.org/content ... 2/11/science.aax0274](https://www.sciencemag.org/content/366/6482/eaax0274) Shiyu Zhu et al. 12 December 2019, *Science*.

2. Quantized Majorana conductance www.nature.com/articles/nature26142 Hao Zhang et al. 28 March 2018, *Nature*.

3. Zero-energy vortex bound state in the superconducting topological surface state of Fe(Se,Te) www.nature.com/articles/s41563-019-0397-1 T. Machida, 17 June 2019, *Nature Materials*.

© 2019 Science X Network

Citation: Nearly quantized conductance plateau of vortex mode in an iron-based superconductor (2019, December 31) retrieved 27 April 2024 from <https://phys.org/news/2019-12-quantized-plateau-vortex-mode-iron-based.html>

This document is subject to copyright. Apart from any fair dealing for the purpose of private study or research, no part may be reproduced without the written permission. The content is provided for information purposes only.